

## COMPARISON OF THE SIZE-INDEPENDENT FRACTURE ENERGY OF CONCRETE OBTAINED BY TWO TEST METHODS

HÉCTOR CIFUENTES<sup>†\*</sup>, MARÍA ALCALDE<sup>†</sup> AND FERNANDO MEDINA

<sup>†</sup> Escuela Técnica Superior de Ingeniería, Universidad de Sevilla  
Camino de los Descubrimientos s/n, 41092 Sevilla, Spain  
e-mail: bulte@us.es, www.esi.us.es

**Key words:** Concrete, Size Effect, Boundary Effect, Size-Independent Fracture Energy, Transition Length

**Abstract:** Three-point bend tests have been performed using two most popular methods available in the literature for determining the size-independent specific fracture energy of concrete. It is shown that despite the different physical interpretations underlying these two methods, they both give nearly the same value.

### 1 INTRODUCTION

The most commonly used method for measuring the fracture energy is the work-of-fracture method recommended by RILEM [1]. However, the specific fracture energy so determined has been shown by several authors [2-5] to depend on the shape and size of the test specimen. The reasons for this variability the size of the specimen are a subject of ongoing investigations [6-9].

Several authors have proposed new methods or modifications of the RILEM method to obtain size-independent specific fracture energy of concrete. The two most popular methods for measuring the size-independent fracture energy of concrete are based on the local fracture energy model of Hu et al. [4,10] and the proposal of Elices et al. [11-13] that provides experimental corrections to avoid energy dissipations. However, there is still no agreement as to which of these methods to use.

The aim of this paper is to provide an evaluation of these two methods based on independent tests in order to see whether the values of the size-independent fracture energy determined by them are the same or not.

### 2 THEORETICAL BACKGROUND

#### 2.1 Boundary effect method (BEM)

Hu et al. [4] argued that the effect of the free boundary of the specimen is felt in the fracture process zone (FPZ) of concrete. The energy required to create a fresh crack decreases as the crack approaches the free boundary [14] of the specimen. This change in the local fracture energy ( $g_f$ ) is represented by a bi-linear approximation, as shown in Figure 1. The transition from the size-independent specific fracture energy of concrete ( $G_F$ ) to the rapid decrease occurs at the transition ligament length ( $a_l$ ), which depends on the both the material properties and specimen size and shape [10]. The measured RILEM fracture energy ( $G_f$ ) represents the average of the local fracture energy function over the ligament area (dashed line in Figure 1). The relationship between all the involved variables is given by

$$G_f(a, D) = \begin{cases} G_F \left[ 1 - \frac{a_l/D}{2(1-a/D)} \right]; & 1-a/D > a_l/D \\ G_F \frac{1-a/D}{2a_l/D}; & 1-a/D \leq a_l/D \end{cases} \quad (1)$$

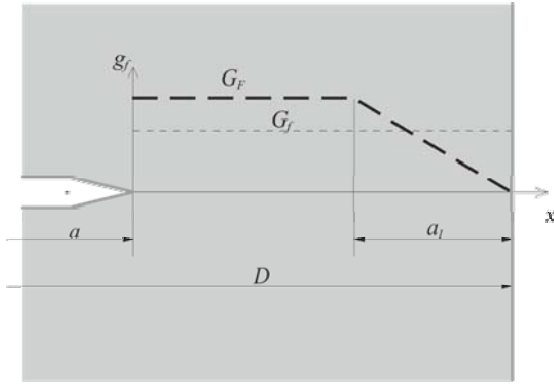


**Figure 1:** Local fracture energy model of Hu and Wittmann.

To obtain the values of  $G_F$  and  $a_l$  for a concrete mix, the RILEM fracture energy of at least four specimens of the same size but different notch depths must be previously determined [10]. Application of equation (1) to each different notch depth specimen gives an over-determined system of linear equations in  $G_F$  and  $a_l$ . This system must be solved by a least squares method for the best estimates of  $G_F$  and  $a_l$  [14].

Abdalla and Karihaloo [15-16] showed that the same size-independent specific fracture energy can also be obtained by testing only two specimens of the same size but with notches which are well separated (e.g.,  $a/D = 0.05$  and  $0.50$ ). This greatly simplifies the determination of  $G_F$ , especially when large specimens are required for testing. This simplified method (SBEM) is one of the methods used in the present paper to achieve the first aim.

## 2.2 Method proposed by Elices et al. ( $P$ - $\delta$ tail)

Elices, Planas and Guinea [11-13] identified several sources of energy dissipation that may influence the measurement of  $G_F$  using the RILEM method. The most important of these is the curtailment of the tail part of the load-displacement curve ( $P$ - $\delta$ ) in a three-point bend test. They proposed some corrections in order to avoid several sources of energy dissipation, such as the adjustment of the initial stiffness of the  $P$ - $\delta$  curve, the adequate design of supports and the system load, and the estimation of the non-measured energy

dissipation near the very end of the test. This last energy dissipation is akin to the curtailment of the tail of the  $P$ - $\delta$  curve.

To estimate this non-measured work of fracture ( $W_{nm1} + W_{nm2}$ ) (Figure 3) when the test is terminated at very low loads, it is necessary to model the beam behavior when the cohesive crack closely approaches the free surface [11]. For cohesive materials and specimens where the weight is compensated, the last phase of a stable three-point bend test can be modelled following the rigid-body kinematics (Figure 2) used by Petersson [17].

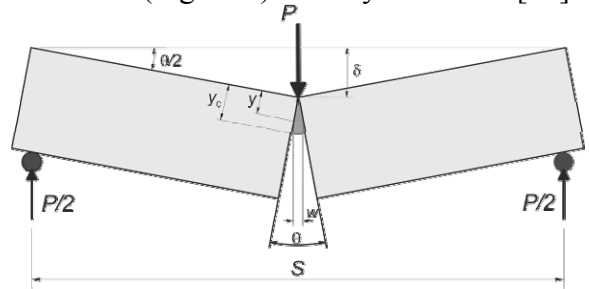


**Figure 2:** Rigid-body model of the behavior of the specimen at the end of the test.

Taking into account the geometrical relationships provided by the rigid-body model, the non-measured fracture energy of the three-point bend test (Figure 3) can be estimated as [11]:

$$W_{nm} = W_{nm1} + W_{nm2} = \frac{2A}{\delta_u} \quad (2)$$

where  $A$  is an experimental coefficient of adjustment of the  $P$ - $\delta$  tail and  $\delta_u$  is the last recorded mid-span deflection of the specimen at the termination of the test (Figure 3).

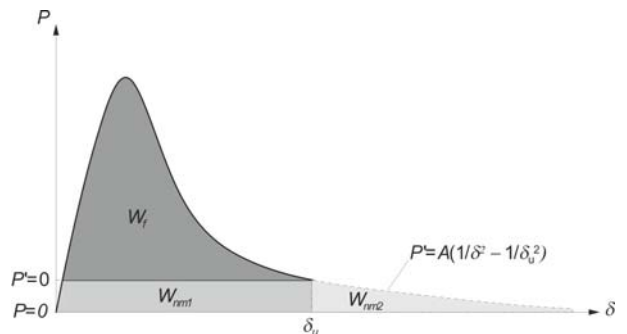


**Figure 3:**  $P$ - $\delta$  curve in a three-point bend test and the measured ( $W_f$ ) and non-measured ( $W_{nm1} + W_{nm2}$ ) work of fracture.

Once the non-measured work of fracture has been estimated, the size-independent fracture energy of concrete can be calculated as [11]:

$$G_F = \frac{\int_0^{\delta_u} Pd\delta + 2A/\delta_u}{b(D-a)} \quad (3)$$

### 3 COMPARISON OF THE TWO MAIN METHODS FOR MEASURING THE SIZE-INDEPENDENT FRACTURE ENERGY OF CONCRETE

#### 3.1 Experimental procedure

To compare the values of the size-independent fracture energy obtained using the two methods described above an experimental program was carried out. Prismatic notched specimens were subjected to three-point bending according to the experimental requirements of each method. Three types of notched beams were manufactured. The beams identified as TFE05 and TFE005 were used to obtain the true fracture energy of concrete by means of the simplified local fracture energy method of Karihaloo et al. [16]. In contrast, beams identifies as SWC05 specimens were used to determine the true fracture energy according to Elices et al. [11]. Table 1 shows the geometrical dimensions of all specimens according to Figure 4.

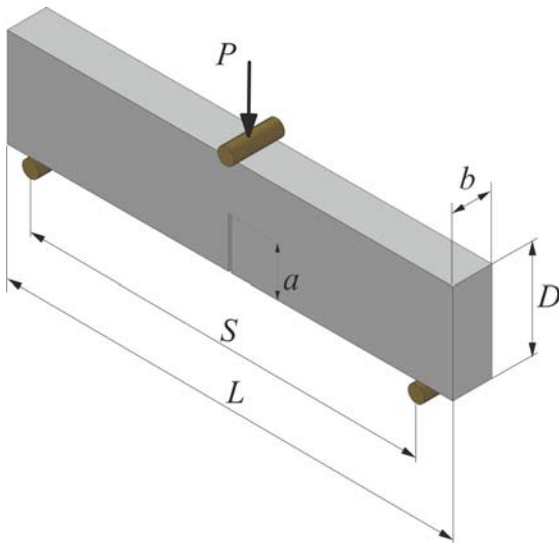


Figure 4: Geometry of the notched specimens.

Table 1: Geometrical properties of the notched specimens in mm

Spec.	<i>D</i>	<i>B</i>	<i>S</i>	<i>L</i>	<i>a</i>
TFE005	120	60	480	540	6
TFE05	120	60	480	540	60
SWC05	120	60	480	540	60

Four samples were tested for each type of specimen. The initial correction for any crushing of the concrete at the supports was made for all specimens. The TFE05 and TFE005 specimens were tested according to the RILEM procedure and the self-weight was no compensated. Figure 5 shows a picture of a three-point bend test of these specimens (bottom) and its instrumentation (top).

The SWC05 specimens were subjected to three-point bend tests with the indicated self-weight compensation (Figure 6). In these specimens the displacement at which the test was stopped was 3.5 mm.

All tests were performed in a closed-loop servo-hydraulic dynamic testing machine with the crack mouth opening displacement (*CMOD*) control. The *CMOD* displacement was measured with a clip gauge, and a linearly varying displacement transducer (LVDT) was used to measure the vertical displacement at mid-point (Figure 5). A reference frame was used to fix the LVDT to the top of the specimen so only the vertical displacement by deformations of the specimen was measured. The load-*CMOD* and load-displacement curves for all specimens were recorded. Loading was applied at a rate, so that the total time of the test was at least twenty minutes.

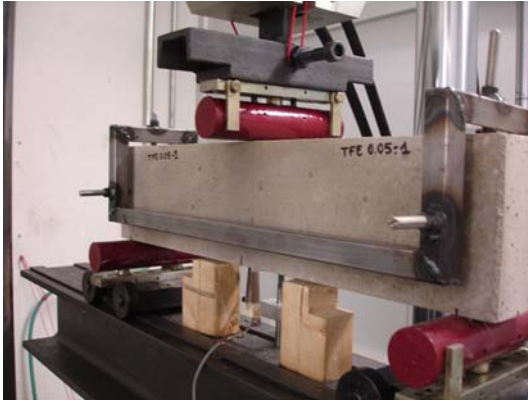


**Figure 5:** Three-point bend test of the TFE05 specimens (bottom) and its instrumentation (top).

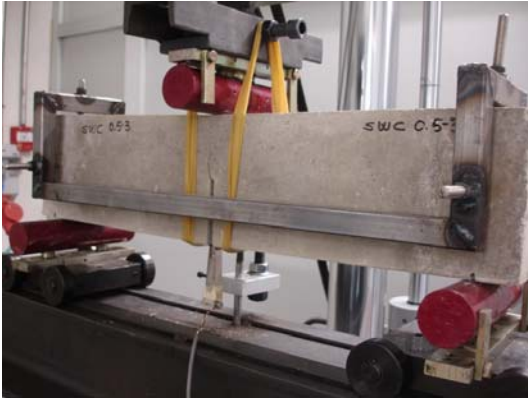


**Figure 6:** Three-point bend test of SWC05 specimens with weight compensation.

### 3.2 Concrete

All specimens were cast from a single concrete mix. The mix proportions by weight of sand/gravel/cement/water were 1.4/3.5/1/0.4. The sand and gravel were siliceous aggregates with a maximum size of 8 mm graded according to the Fuller method. Starter notches were made by a diamond saw (blade thickness 3 mm). The specimen

preparation process was strictly controlled to minimize scatter in the test results.

Compressive tests were carried out on cylindrical specimens of 150×300 mm (diameter×height). The Young modulus was estimated from the  $P-CMOD$  curve, according to the procedure indicated in [18]. Brazilian tests were also carried out on cylindrical specimens of the same size to obtain the split tensile strength of concrete mix. Table 2 shows the mechanical properties of concrete.

**Table 2:** Mechanical properties of concrete

Compressive strength, $f_c$ (MPa)	$36.9 \pm 6\%$
Splitting tensile strength, $f_{ti}$ (MPa)	$3.1 \pm 13\%$
Modulus of rupture, $f_f$ (MPa)	$4.6 \pm 1\%$
Young's modulus, $E_c$ (GPa)	$28.2 \pm 11\%$

### 3.3 Results

Table 3 shows the average values of the fracture energy obtained from the three-point bend tests of TFE005 and TFE05 specimens according to the RILEM procedure [1]. The notations used in the table are: the maximum load obtained from tests ( $P_{max}$ ), the self-weight of specimens ( $m$ ), the vertical displacement at the end of the test ( $\delta_u$ ), the maximum load corrected according to the self-weight of the specimen ( $P'_{max}$ ), the work of fracture measured from the  $P-\delta$  curve ( $W_f$ ), the total work of fracture considering the self-weight correction ( $W_{fT}$ ), the ligament area ( $A_{lig}$ ) and the RILEM specific fracture energy ( $G_f$ ).

Table 4 shows the SWC05 specimen results for determining  $G_F$  according to the adjustment for the tail curtailment, where:  $\delta_0$  is the displacement considered as the initial point for adjusting the tail of the curve,  $A$  is the constant of adjustment,  $W_{nm}$  is the non-measured work of fracture and  $G_F$  is the size-independent specific fracture energy (equation 3).

The comparison of  $G_f$  values obtained for TFE005 and TFE05 specimens clearly reveals the size dependency of the specific fracture energy according to RILEM procedure. Applying the simplified method of Karihaloo et al. [15] (equation (1)) to these results, the size-independent fracture energy of concrete

and the transition length were obtained (Table 5).

**Table 3:** RILEM fracture energy in TFE specimens

Specimen	TFE005	TFE05
$P_{max}$ (N)	4733 $\pm$ 4%	1332 $\pm$ 4%
$m$ (kg)	9.6 $\pm$ 2%	9.6 $\pm$ 1%
$\delta_u$ (mm)	1.41 $\pm$ 4%	1.35 $\pm$ 1%
$P'_{max}$ (N)	4775 $\pm$ 4%	1358 $\pm$ 4%
$W_f$ (Nmm)	797.7 $\pm$ 12%	333.5 $\pm$ 5%
$W_{fT}$ (Nmm)	915.4 $\pm$ 11%	448.3 $\pm$ 4%
$A_{lig}$ (mm <sup>2</sup> )	6840	3600
$G_f$ (N/m)	133.8 $\pm$ 11%	124.5 $\pm$ 4%

**Table 4:** Size-independent fracture energy from SWC specimens

SWC05	1	2	3	4
$P_{max}$ (N)	1444	1585	1410	1547
$m$ (kg)	9.4	9.8	9.7	9.7
$\delta_0$ (mm)	2.1	2.1	2.1	2.1
$\delta_u$ (mm)	3.5	3.4	3.6	3.5
$A$ (Nmm <sup>2</sup> )	84.4	172.3	98.1	113.8
$W_f$ (Nmm)	518.6	484.4	390.3	430.3
$W_{nm}$ (Nmm)	48.3	99.9	56.6	65.5
$A_{lig}$ (mm <sup>2</sup> )	3600	3600	3600	3600
$G_F$ (N/m)	157.5	162.3	123.9	137.7

The specific fracture energy ( $G_F$ ) determined with this method is directly the size-independent fracture energy of concrete. So the value of the true fracture energy obtained with this method is the average value for all specimens SWC05 (Table 5).

**Table 5:** Size-independent fracture energy of concrete obtained by each method

Method	$G_F$ (N/m)	$a_l$ (mm)
SBEM	144.2	16.4
$P$ - $\delta$ tail	145.4 $\pm$ 12%	-

Comparing the  $G_F$  results given by the two competing methods, it is clear that they both give almost the same size-independent fracture energy. Although these two methods use different experimental procedures, it is not surprising that they lead to the same size-independent fracture energy, as had been conjectured by Karihaloo et al. [15]. Both these methods essentially recognise that the

local fracture energy is not constant over the FPZ. The local fracture energy model allows for this variation directly when the crack approaches the back free boundary surface of the specimen which occurs towards the end of the test [19]. On the other hand, the method of Elices et al. takes this into account indirectly by adjusting the work of fracture for the unmeasured tail of the  $P$ - $\delta$  curve that also corresponds to the final part of the test [11].

## 5 CONCLUSIONS

A comparison of the two main methods used to measure the size-independent fracture energy of concrete has been carried out using independent experimental results. The value of the fracture energy obtained by both methods was practically identical. This is not surprising, as had been anticipated by Abdalla and Karihaloo [15]. Although these two use slightly different experimental techniques, they both essentially include the influence of the back free boundary of the specimen on the FPZ when the propagating crack approaches at the end of the test (also reflected in the tail of the  $P$ - $\delta$  diagram). It is therefore concluded that either method can be used to obtain a unique value of the size-independent fracture energy of concrete.

During the presentation a new method will also be briefly described to estimate the size-independent fracture energy from the measured fracture energy of three geometrically similar specimens and one extra specimen with a notch to depth ratio different from these three

## REFERENCES

- [1] RILEM TCM-85, Determination of the fracture energy of mortar and concrete by means of three-point bend tests on notched beams. Materials and Structures, 1985. 18(106): p. 287-290.
- [2] Bazant, Z.P. and M.T. Kazemi, Size dependence of concrete fracture energy determined by RILEM work-of-fracture method. International Journal of Fracture, 1991. 51: p. 121-138.
- [3] Nallathambi, P., B.L. Karihaloo, and B.S.

- Heaton, Various size effect in fracture of concrete. *Cement and Concrete Composites*, 1985. 15: p. 117-126.
- [4] Hu, X. and F. Wittmann, Fracture energy and fracture process zone. *Materials and Structures*, 1992. 25: p. 319-326.
- [5] Mindess, S., The effect of specimen size on the fracture energy of concrete. *Cement and Concrete Research*, 1984. 14: p. 431-436.
- [6] Vydra, V., K. Trtík, and F. Vodák, Size independent fracture energy of concrete. *Construction and Building Materials*, 2012. 26(1): p. 357-361.
- [7] Zhao, Z., S. Kwon, and S. Shah, Effect of specimen size on fracture energy and softening curve of concrete: Part I. Experiments and fracture energy. *Cement and Concrete Research*, 2008. 38(8-9): p. 1049-1060.
- [8] Kwon, S., Z. Zhao, and S. Shah, Effect of specimen size on fracture energy and softening curve of concrete: Part II. Inverse analysis and softening curve. *Cement and Concrete Research*, 2008. 38(8-9): p. 1061-1069.
- [9] Hu, X., Size effect on tensile softening relation. *Materials and Structures*, 2010. 44(1): p. 129-138.
- [10] Hu, X. and F. Wittmann, Size effect on toughness induced by crack close to free surface. *Engineering Fracture Mechanics*, 2000. 65: p. 209-221.
- [11] Elices, M., G.V. Guinea, and J. Planas, Measurement of the fracture energy using three-point bend tests: Part 3—Influence of cutting the  $P-\delta$  tail. *Materials and Structures*, 1992. 25(6): p. 137-163.
- [12] Guinea, G.V., J. Planas, and M. Elices, Measurement of the fracture energy using three-point bend tests: Part 1—Influence of experimental procedures. *Materials and Structures*, 1992. 25(4): p. 212-218.
- [13] Planas, J., M. Elices, and G.V. Guinea, Measurement of the fracture energy using three-point bend tests: Part 2—Influence of bulk energy dissipation. *Materials and Structures*, 1992. 25(5): p. 305-312.
- [14] Hu, X., Influence of fracture process zone height on fracture energy of concrete. *Cement and Concrete Research*, 2004. 34(8): p. 1321-1330.
- [15] Karihaloo, B.L., H.M. Abdalla, and T. Imjai, A simple method for determining the true specific fracture energy of concrete. *Magazine of Concrete Research*, 2003. 55(5): p. 471-481.
- [16] Abdalla, H.M. and B.L. Karihaloo, Determination of size-independent specific fracture energy of concrete from three-point bend and wedge splitting tests. *Magazine of Concrete Research*, 2003. 55(2): p. 133-141.
- [17] Petersson, P.E., Fracture energy of concrete: Method of determination. *Cement and Concrete Research*, 1980. 10: p. 78-89.
- [18] TC 187-SOC, Final Report of RILEM Technical Committee TC 187-SOC: 'Experimental determination of the stress-crack opening curve for concrete in tension'. 2007.
- [19] Hu, X.Z. and K. Duan, Mechanism behind the size effect phenomenon. *Journal of Engineering Mechanics (ASCE)*, 2010. 136: p. 60-68.